Cyclin dependent kinase 1-dependent activation of APC/C ubiquitin ligase

Kazuyuki Fujimitsu[1], Margaret Grimaldi[1] and Hiroyuki Yamano[1*]

[1]*Cell Cycle Control Group, UCL Cancer Institute, University College London, London, WC1E 6DD, UK*

[*]Corresponding author. Email: h.yamano@ucl.ac.uk

Abstract

Error-free genome duplication and segregation are ensured through the timely activation of ubiquitylation enzymes. The anaphase-promoting complex/cyclosome (APC/C), a multi-subunit E3 ubiquitin ligase, is regulated by phosphorylation. However the mechanism remains elusive. Using systematic reconstitution and analysis of vertebrate APC/Cs under physiological conditions, we show how cyclin-dependent kinase 1 (CDK1) activates the APC/C through coordinated phosphorylation between Apc3 and Apc1. Phosphorylation of the loop domains by p9/Cks2 (CDK regulatory subunit)-CDK1 controlled loading of co-activator Cdc20 onto APC/C. A phosphomimetic mutation introduced into Apc1 allowed Cdc20 to increase APC/C activity in interphase. These results define a previously unrecognised subunit-subunit communication over a distance and the functional consequences of CDK phosphorylation. Cdc20 is a potential therapeutic target and our findings may facilitate the development of specific inhibitors.

One Sentence Summary:

CDK1-dependent coordinated phosphorylation operating between Apc3 and Apc1 leads to activation of the APC/C ubiquitin ligase and trigger anaphase.

Main Text:

Many biological processes are regulated by post-translational modifications such as phosphorylation and ubiquitylation. The anaphase-promoting complex or cyclosome (APC/C) (*1-3*) is an unusually large multi-subunit (>13) enzyme and key component of the cellular machinery that regulates cell cycle progression and genome stability by catalysing ubiquitylation of regulatory proteins such as securin and cyclin B leading to their proteolysis (*4-6*). The activity of the APC/C controls mitotic exit. Anti-microtubule agents that disrupt spindle function are effective in the clinic because they cause mitotic delay, which triggers apoptosis of cancer cells. However, microtubules have key roles in neuronal functions, so the development of agents that block cells in mitosis without altering microtubules is important. One way to do this would be to target the APC/C (*7-11*). Mitotic kinases, including cyclin-dependent kinase 1 (CDK1), phosphorylate vertebrate APC/C at more than 50 sites during mitosis (*12, 13*) and the co-activator subunit Cdc20 preferentially binds to and activates phosphorylated APC/C (*14-16*). However, all the evidence in vertebrates that CDK1 activates the APC/C comes from in vitro phosphorylation/ubiquitylation studies, and no mutagenesis of these sites has been done. To elucidate how CDK phosphorylates and activates the APC/C, we reconstituted recombinant *Xenopus* APC/C by simultaneous co-expression of all the subunits using an advanced baculovirus/insect cell expression system (*17, 18*) (fig. S1, A and B). The activities of purified APC/C were assessed under physiological conditions in a cyclin B destruction assay

reconstituted in *Xenopus* egg extracts. Incubation of reconstituted recombinant APC/C in extract from which endogenous APC/C was depleted (ΔAPC/C+APC/C) revealed that the reconstituted APC/C was active and degraded a substrate, cyclin B (fig. S1, C and D). The purified APC/C also ubiquitylated and degraded substrates in a Cdh1-dependent manner (fig. S1, E and F). Cdh1, an alternative co-activator of the APC/C in G1, activates the APC/C independently of subunit phosphorylation. These results indicated that our reconstituted *Xenopus* APC/C was functional. We mutated all conserved (between *Xenopus* and humans) CDK consensus phosphorylation sites of each individual subunit to alanine (A) and made mutant APC/Cs, one subunit at a time (table S1). The cyclin destruction assay in anaphase revealed that only APC/$C^{Apc1\text{-}15A}$ (the reconstituted APC/C containing mutated 15 CDK sites on Apc1) and APC/$C^{Apc3\text{-}12A}$ mutants showed decreased activity (Fig. 1A and fig. S2A). The integrity of the APC/C was confirmed in a Cdh1-dependent assay. The activities of APC/$C^{Apc3\text{-}12A}$ and APC/$C^{Apc1\text{-}15A}$ were similar to that of WT, albeit APC/$C^{Apc1\text{-}15A}$ showed reduced activity (fig. S2, B and C). These results prompted us to further investigate Apc3 and Apc1.

In the absence of a co-activator, the APC/C is always inactive. We examined the binding of Cdc20 to APC/$C^{Apc3\text{-}12A}$ and APC/$C^{Apc1\text{-}15A}$. We confirmed that APC/C^{WT} bound Cdc20 in a cell-cycle-dependent manner; binding was low in interphase and high in anaphase (Fig. 1B). Consistent with the destruction assay in anaphase, APC/$C^{Apc3\text{-}12A}$ showed a lower affinity for Cdc20 than APC/C^{WT} (Fig. 1B). Cdc20 also failed to bind APC/$C^{Apc1\text{-}15A}$ in anaphase (Fig. 1C). No shift in the electrophoretic band containing Apc3 or Apc1 was detected in anaphase extract for APC/$C^{Apc3\text{-}12A}$ or APC/$C^{Apc1\text{-}15A}$ respectively (Fig. 1, B and C), consistent with the mutated CDK sites no longer being phosphorylated. This was confirmed by in vitro phosphorylation using purified CDK1-cyclin B (Fig. 1D).

Why is the phosphorylation of two subunits, Apc3 and Apc1, of particular importance? Cdc20 directly binds the Apc3 subunit through the C-terminal IR (Ile-Arg) motif of Cdc20 (*19*). However, because the sites phosphorylated by CDK (except S567) are distant from tetratricopeptide repeat (TPR) motifs implicated in engaging co-activator IR motifs, the role of CDK might not be simply to increase the affinity of Apc3 to Cdc20 by phosphorylation. The twelve CDK sites on Apc3 are widely spread throughout the protein (Fig. 2A). To understand the CDK-driven APC/C activation mechanism, we constructed several mutant APC/Cs carrying CDK mutations in Apc3 and tested the activities (fig. S3). Mutations within the dimerization domain (T68A/S150A) or adjacent to the IR-binding domain (S567A) had no impact on APC/C activity. In contrast, CDK mutations in the predicted loop domain (Apc3-7A, -8A and -9A) reduced APC/C activity in anaphase as seen with Apc3-12A, highlighting the importance of loop domain phosphorylation (fig. S3, A to C). APC/$C^{Apc3\text{-}7A}$, APC/$C^{Apc3\text{-}8A}$ and APC/$C^{Apc3\text{-}9A}$ mutants also showed reduced Cdc20 binding in anaphase extract (Fig. 2B, lanes 16-20). Although the predicted loop domain comprises approximately 280-residue-sequences conserved among vertebrates (fig. S4), the function remains uncharacterised. Complexes of the *Xenopus* p9 protein (Suc1 or Cks1/2 in other organisms) (*20*) with CDK1 only bound to WT APC/C when phosphorylated in anaphase, but not interphase (Fig. 2B and fig. S5A). The Apc3 loop mutants failed to bind p9-CDK1 (Fig. 2B, lanes 17-19), consistent with findings that p9 is required for phosphorylation of Apc3 in anaphase (*15, 21, 22*). The Suc1/Cks family of proteins may recognise CDK sites and stimulate phosphorylation-dependent CDK signalling (*23, 24*). Thus, CDK phosphorylation of the loop domain in Apc3 might recruit p9-CDK1 and lead to phosphorylation of Apc1, another key CDK target in the APC/C. Furthermore, we examined the physical interaction between Apc3 fragments and p9. A bacterially purified fragment from the

loop domain (residues 202-342) bound to p9 in mitotic egg extracts, whereas the same fragment with CDK site mutations did not bind p9 (fig. S5B). These results indicate that Apc3 functions as a scaffold for p9-CDK1 through the loop domain.

To investigate the mechanism of Apc1 phosphorylation-dependent APC/C activation, we sought to identify key phosphorylation sites on Apc1 (Fig. 2C). We made a series of mutant Apc1-APC/Cs (fig. S6A). The construct with CDK mutations in a predicted flexible loop domain (Apc1-7A) reduced cyclin destruction in anaphase whereas all the others showed similar more rapid cyclin B destruction kinetics (fig. S6, B and C and fig. S7). In a Cdh1-supplemented destruction assay, all the constructs showed similar activity to APC/C^{WT} (fig. S6, D and E). Cdc20 loading was also assessed. Cdc20 loading to the APC/C in anaphase was abolished by the 7A mutation (Fig. 2D, lane 25) whereas in interphase extract APC/$C^{Apc1\text{-}7A}$ retained basal Cdc20-binding as seen with APC/C^{WT} (Fig. 2D, lanes 15 and 18). These results indicate that phosphorylation of the loop domain mutated in APC/$C^{Apc1\text{-}7A}$ is necessary for Cdc20-binding and subsequent APC/C activation. To verify the relationship between Apc1 and Apc3 phosphorylation, we raised a phospho-specific antibody that bound to the Apc1 loop domain only when S314 and S318 were phosphorylated (fig. S8). The specificity of this antibody was verified with bacterially produced peptide containing Apc1 residues 294-399 (hereafter $Apc1^{loop}$) incubated either in anaphase or interphase extract (fig. S8, A and C). The CDK sites on $Apc1^{loop}$ were barely phosphorylated in Apc3 CDK site mutant APC/Cs whereas they were highly phosphorylated in APC/C^{WT} in anaphase (Fig. 2E). Thus CDK phosphorylation in $Apc1^{loop}$ appears to depend upon Apc3 phosphorylation, highlighting that Apc3 influences Apc1 by recruitment of p9-CDK1.

Because both APC/$C^{Apc1\text{-}7A}$ and APC/$C^{Apc3\text{-}9A}$ retain some APC/C-dependent cyclin destruction activity, we tested the phenotype of the double mutant. APC/$C^{Apc3\text{-}9A/Apc1\text{-}7A}$ appeared more deficient in cyclin destruction than APC/$C^{Apc1\text{-}7A}$ or APC/$C^{Apc3\text{-}9A}$ alone (Fig. 3A and fig. S9). APC/$C^{Apc3\text{-}9A/Apc1\text{-}7A}$ failed to destroy cyclin A and securin as well (Fig. 3B). We also investigated the activity of APC/$C^{Apc3\text{-}9A/Apc1\text{-}7A}$ using a "cycling" frog egg extract where the endogenous APC/C is replaced by APC/$C^{Apc3\text{-}9A/Apc1\text{-}7A}$ (fig. S10). Unlike WT, APC/$C^{Apc3\text{-}9A/Apc1\text{-}7A}$ could not support cyclin or securin destruction. Consistently, an in vitro phosphorylated APC/$C^{Apc3\text{-}9A/Apc1\text{-}7A}$ showed less activity than APC/C^{WT} in an in vitro ubiquitylation assay (Fig. 3C and fig. S11). Thus, phosphorylation of Apc1 and Apc3 subunits is crucial for APC/C activation. However, it is conceivable that phosphorylation of other subunits or an alternative pathway (e.g. phosphatases) might be involved to some extent in vivo (Fig. 3A and fig. S12). Nevertheless, if phosphorylation of Apc3 and Apc1 is important, an Apc1 phosphomimetic mutation (Asp: D) might bypass both Apc3 and Apc1 phosphorylation making CDK phosphorylation dispensable. We tested this in interphase extracts, in which neither CDK nor APC/C-Cdc20 is active. If Apc1 had the phosphomimetic mutation (7D), the APC/C was activated by Cdc20 even in interphase, triggering cyclin B destruction, albeit with slower kinetics than those observed with APC/C in anaphase (Fig. 3D and fig. S13A). The Apc1-7D gain-of-function phenotype was further confirmed by a "cycling" extract and an in vitro ubiquitylation assay (fig. S13, B and C). These results indicate that the phosphorylation status of the $Apc1^{loop}$ is a crucial determinant of Cdc20 loading and activation of the APC/C.

We found that in co-immunoprecipitation assays, $Apc1^{loop\text{-}7A}$ ($Apc1^{loop}$ carrying 7A mutation) bound to the APC/C in anaphase extract whereas WT $Apc1^{loop}$ fragment did not (Fig. 3E). Conversely, these phosphomimetic mutations abolished the interaction with the APC/C (fig.

S14), highlighting that interaction of the Apc1^{loop} with the APC/C depends on its phosphorylation status. In the atomic structure of human APC/C$^{Cdh1.Emi1}$ determined using cryo-EM (*25*), residues corresponding to the Apc1^{loop} are disordered and not observed in the EM density map. However given the putative location of Apc1^{loop} proximal to Cdh1^{NTD} (*25*) (fig. S15), phosphorylation-dependent structural changes of Apc1^{loop} could influence the APC/C binding sites for the NTD of co-activator located on Apc8 (*25, 26*), the PC domain of Apc1 (*25*), and Apc6 (*26*). Consistent with this idea, Cdc20-NTD binding was reduced in APC/C$^{Apc1\text{-}7A}$, compared with APC/C^{WT} (Fig. 3F).

Our results reveal the presence and importance of the coordinated phosphorylation of Apc3 and Apc1 within the APC/C complex for the control of the APC/C in mitosis (Fig. 4). Extended flexible loops in both subunits have a key role; one acts as a scaffold of p9-CDK1 and the other for phosphorylation-dependent interaction with Cdc20-NTD. Previous studies in yeast and Drosophila provide in vivo evidence that CDK1 phosphorylation of the APC/C is required for its mitotic activity (*22, 27, 28*). Our present study extends past findings (*13-16, 22*) and uncovers the mechanistic insight and the functional consequences of APC/C phosphorylation in vertebrates. Cdc20 (not Cdh1, which is a tumour suppressor (*29*)) is a promising anti-cancer therapeutic target (*7, 8, 10, 30*). The Apc1^{loop} may provide a target for strategies to specifically inhibit APC/C-Cdc20.

References and Notes

1. V. Sudakin *et al.*, *Mol Biol Cell* **6**, 185-197 (1995).
2. S. Irniger, S. Piatti, C. Michaelis, K. Nasmyth, *Cell* **81**, 269-278 (1995).
3. R. W. King *et al.*, *Cell* **81**, 279-288 (1995).
4. I. Primorac, A. Musacchio, *J Cell Biol* **201**, 177-189 (2013).
5. L. Chang, D. Barford, *Curr. Opin. Struct. Biol.,* **29C**, 1-9 (2014).

6. J. Pines, *Nat Rev Mol Cell Biol* **12**, 427-438 (2011).
7. H. C. Huang, J. Shi, J. D. Orth, T. J. Mitchison, *Cancer Cell* **16**, 347-358 (2009).
8. E. Manchado *et al.*, *Cancer Cell* **18**, 641-654 (2010).
9. X. Zeng *et al.*, *Cancer Cell* **18**, 382-395 (2010).
10. K. L. Sackton *et al.*, *Nature* **514**, 646-649 (2014).
11. K. E. Gascoigne, S. S. Taylor, *Cancer Cell* **14**, 111-122 (2008).
12. J. A. Steen *et al.*, *Proc. Natl. Acad. Sci. USA.* **105**, 6069-6074 (2008).
13. C. Kraft *et al.*, *EMBO J* **22**, 6598-6609 (2003).
14. E. R. Kramer, N. Scheuringer, A. V. Podtelejnikov, M. Mann, J. M. Peters, *Mol Biol Cell* **11**, 1555-1569 (2000).
15. M. Shteinberg, A. Hershko, *Biochem Biophys Res Commun.* **257**, 12-18 (1999).
16. G. Fang, H. Yu, M. W. Kirschner, *Mol Cell* **2**, 163-171 (1998).
17. Z. Zhang *et al.*, *Biochem J.* **449**, 365-371 (2013).
18. I. Berger, D. J. Fitzgerald, T. J. Richmond, *Nat Biotechnol.* **22**, 1583-1587 (2004).
19. M. E. Matyskiela, D. O. Morgan, *Mol Cell* **34**, 68-80 (2009).
20. D. Patra, W. G. Dunphy, *Genes Dev.* **10**, 1503-1515 (1996).
21. D. Patra, W. G. Dunphy, *Genes Dev.* **12**, 2549-2559 (1998).
22. A. D. Rudner, A. W. Murray, *J Cell Biol*.**149**, 1377-1390 (2000).
23. M. Koivomagi *et al.*, *Nat. Struct. Mol. Biol.* **20**, 1415-1424 (2013).
24. D. A. McGrath *et al.*, *Nat. Struct. Mol. Biol.* **20**, 1407-1414 (2013).
25. L. Chang, Z. Zhang, J. Yang, S. H. McLaughlin, D. Barford, *Nature* **522**, 450-454 (2015).
26. H. Labit *et al.*, *EMBO J.* **31**, 3351-3362 (2012).
27. N. Lianga *et al.*, *J Cell Biol* **201**, 843-862 (2013).
28. J. Y. Huang, G. Morley, D. Li, M. Whitaker, *J Cell Sci* **120**, 1990-1997 (2007).
29. I. Garcia-Higuera *et al.*, *Nat Cell Biol* **10**, 802-811 (2008).
30. K. E. Gascoigne, S. S. Taylor, *J Cell Sci* **122**, 2579-2585 (2009).

Acknowledgments

We thank J. Gannon for monoclonal anti-Apc3, anti-Cdc20 and anti-pPlx1 antibodies; C. Ellenrieder for anti-p9 antibodies; K. Ohsumi for anti-securin antibodies; J. Endicott for purified CDK1-cyclin B; F. Esashi for helpful advice on affinity purification of antibodies; Z. Zhang and D. Barford for providing the methodology and MultiBac-USER expression vectors, members of the Yamano laboratory for helpful discussion and I. Hagan and F. Uhlmann for critical reading of the manuscript. This work was supported by Marie Curie Cancer Care, Cancer Research UK (C8320/A13586) and Medical Research Council (MR/M010899/1).

Supplementary Materials:

Materials and Methods

Figs. S1 to S15

Tables S1

References (*31-36*)

Figure legends

Figure 1. Effect of phosphorylation of Apc3 and Apc1 on APC/C-Cdc20 activation.

(A) Cyclin destruction assay in *Xenopus* egg extracts. APC/C-depleted extracts (ΔAPC/C) were supplemented with a range of reconstituted APC/Cs with CDK site mutations. Samples taken at indicated time points after addition of cyclin were analysed by SDS-PAGE and autoradiography. Quantification of fig. S2A. The relative cyclin levels are shown, normalized with reference to the intensities found at time 0 for each time point. **(B)** WT APC/C or APC/C$^{Apc3\text{-}12A}$ was incubated with ΔAPC/C interphase or anaphase extract. The APC/C was recovered with anti-Apc3 beads and bound Cdc20 was analysed by SDS–PAGE and immunoblotting. **(C)** Same as **(B)**, but APC/C$^{Apc1\text{-}15A}$ was used. **(D)** Phosphorylation of APC/C$^{Apc3\text{-}12A}$ and APC/C$^{Apc1\text{-}15A}$ by CDK1-cyclin B. Left: WT APC/C or APC/C$^{Apc3\text{-}12A}$ was incubated with CDK1-cyclin B and p9 in the presence of [γ-^{32}P] ATP at 23˚C for indicated minutes. The APC/C was recovered using anti-Apc3 affinity beads, and analysed by SDS-PAGE and autoradiography. Right: Same as left panel but APC/C$^{Apc1\text{-}15A}$ was used.

Figure 2. Interaction of phosphorylation on Apc3 and Apc1 subunits.

(A) Schematic diagram of Apc3. CDK sites shared between *Xenopus* and Human Apc3 are shown in black. **(B)** WT APC/C or Apc3 mutant APC/Cs were incubated with ΔAPC/C interphase or anaphase extracts. The APC/C was recovered with anti-Apc3 beads and bound proteins were analysed by immunoblotting. LC; IgG light chain. **(C)** Schematic diagram of Apc1. CDK sites shared between *Xenopus* and Human Apc1 are shown in black. **(D)** Binding of Cdc20 to APC/C in anaphase. WT APC/C or Apc1 mutant APC/Cs were incubated with ΔAPC/C interphase or anaphase extracts. APC/C was recovered with anti-Apc3 beads and bound proteins were analysed by immunoblotting. **(E)** Phosphorylation of WT or Apc3 mutant APC/Cs incubated in ΔAPC/C extracts and then recovered with anti-Apc3 beads as detected by immunoblotting with pS314pS318 antibody and indicated APC/C antibodies.

Figure 3. Role of CDK phosphorylation in the activation of the APC/C ubiquitin ligase. (A) Cyclin destruction assay in mock or ΔAPC/C anaphase extracts supplemented with APC/C^{WT}, $APC/C^{Apc1\text{-}7A}$, $APC/C^{Apc3\text{-}9A}$ or $APC/C^{Apc3\text{-}9A/Apc1\text{-}7A}$ (fig. S9). Same as Fig. 1A, relative cyclin levels are shown. (**B**) Same as (**A**), but human cyclin A2 or *Xenopus* securin destruction was examined in ΔAPC/C anaphase extract supplemented with WT or Apc3-9A/Apc1-7A double mutant APC/C. (**C**) WT APC/C or $APC/C^{Apc3\text{-}9A/Apc1\text{-}7A}$ was phosphorylated by p9-CDK1-cyclin B. APC/Cs recovered using anti-Apc3 affinity beads were subjected to cyclin B ubiquitylation assay in the presence/absence of Cdc20. ^{35}S-labelled cyclin B was used as substrate. Samples taken at indicated time points were analysed by SDS–PAGE and autoradiography. The APC/Cs used were monitored by anti-Apc3 and anti-Apc5 immunoblotting. **(D)** Cyclin destruction assay in interphase extracts supplemented with APC/C^{WT}, $APC/C^{Apc3\text{-}9A}$ or $APC/C^{Apc3\text{-}9A/Apc1\text{-}7D}$ (fig. S13A). Error bars, s.e.m. from three independent experiments. **(E)** Bacterially purified Flag-

tagged Apc1 fragment (294-399 WT) or its 7A mutant was incubated with interphase or anaphase extract, immunopurified by anti-Flag beads and bound proteins analysed by immunoblotting. **(F)** Interaction of Cdc20 NTD with APC/C^{WT} or APC/$C^{Apc1\text{-}7A}$. APC/C complexes were incubated with Cdc20 NTD (N159-5A) in interphase or anaphase extract depleted of endogenous APC/C and Cdc20 (ΔAPC/C ΔCdc20). APC/C was recovered with anti-Apc3 beads and bound proteins were analysed by immunoblotting.

Figure 4. Proposed model for CDK1 activation of the APC/C. Top: CDK1 phosphorylates the APC/C and stimulates Cdc20 loading and subsequent ubiquitylation catalysis ('active'). Conversely, at the end of mitosis, the APC/C is dephosphorylated by an as-yet-unidentified phosphatase(s), contributing to the inactivation of APC/C-Cdc20. Bottom: CDK1-dependent phosphorylation-relay for activation of the APC/C. p9-CDK1-cyclinB initially phosphorylates the internal loop domain of Apc3, which allows p9 (Cks2) bound CDK1-cyclin B loading to Apc3. p9-CDK1-cyclin B then stimulates phosphorylation of the internal loop domain of Apc1. The loop domain seems to block Cdc20-NTD access to the APC/C (e.g. Apc8) when it is not phosphorylated, but upon phosphorylation, the loop looses its inhibitory function, allowing Cdc20 NTD loading and subsequent ubiquitylation catalysis.

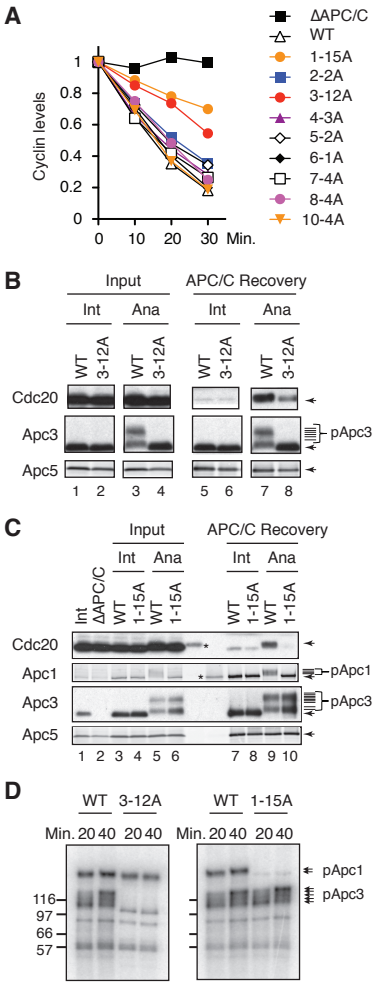

Fujimitsu et al., Figure 1

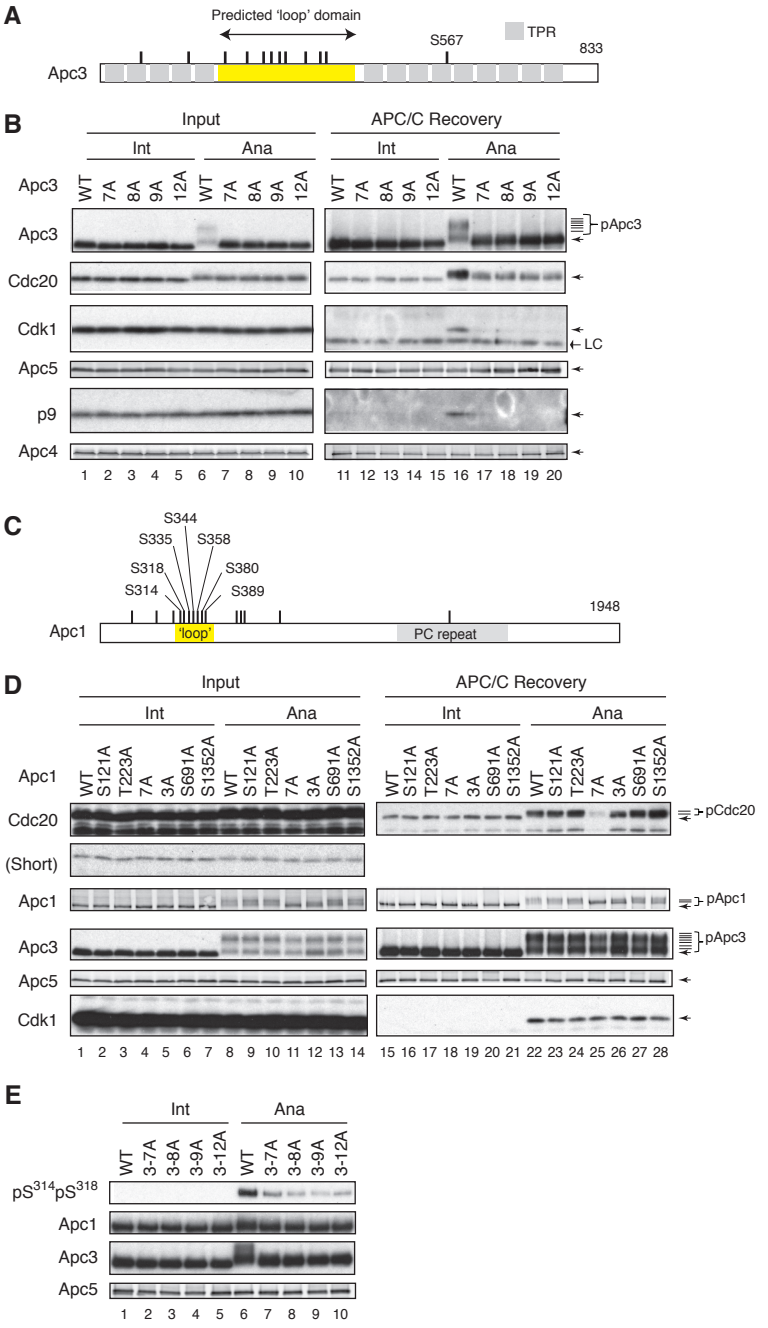

Fujimitsu et al., Figure 2

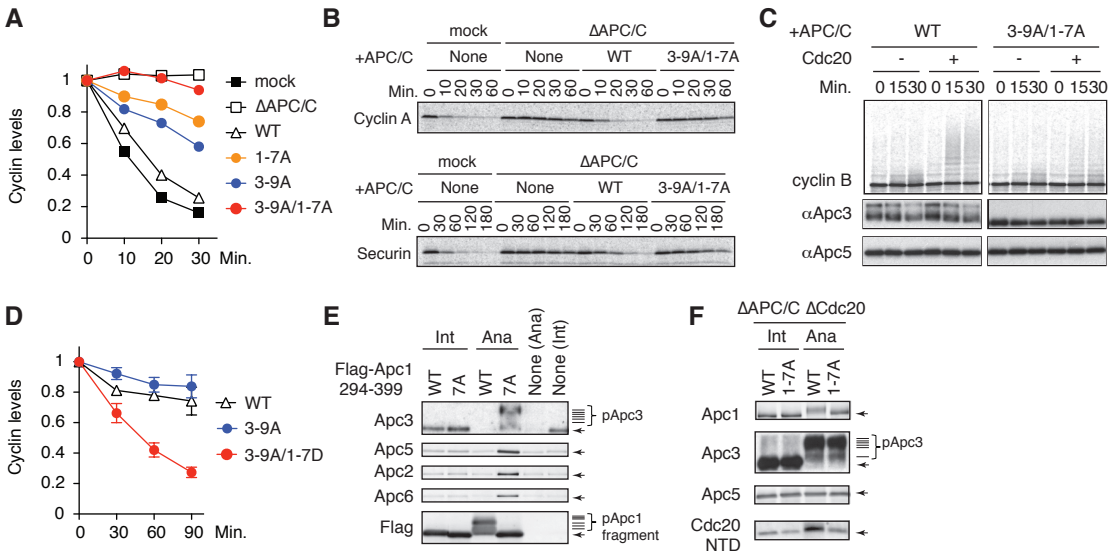

Fujimitsu et al., Figure 3

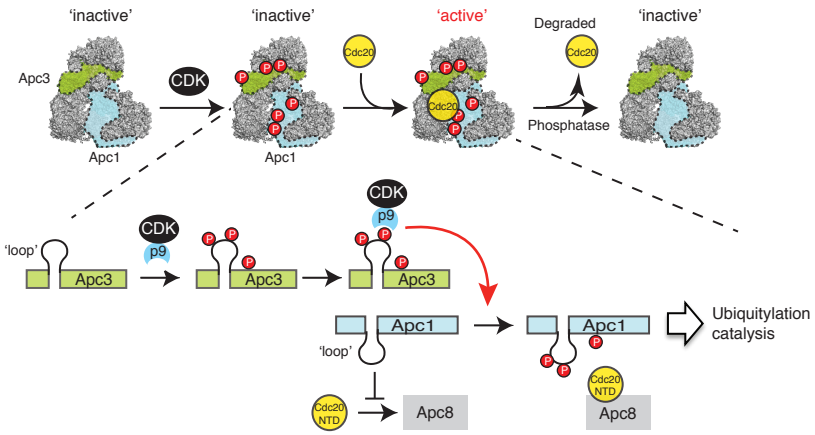

Fujimitsu et al., Figure 4

Supplementary Materials for

Cyclin dependent kinase 1-dependent activation of APC/C ubiquitin ligase

Kazuyuki Fujimitsu, Margaret Grimaldi and Hiroyuki Yamano*

*Corresponding author. Email: h.yamano@ucl.ac.uk

This PDF file includes:

Supplementary Materials:
Materials and Methods

Cloning and expression of recombinant *Xenopus* APC/C (APC/C)

The approach used in this study is based on the modified MultiBac pFBDM and pUCDM system allowing USER ligation-independent cloning (*17, 18*). *Xenopus* APC/C genes, apart from Apc1, were amplified by PCR using *Xenopus laevis* cDNA library. For Apc1, *Xenopus tropicalis* Apc1 was amplified from the IMAGE clone of *Xenopus tropicalis* Apc1 (Source BioScience). All APC/C genes amplified were cloned into pOENmyc vector with polH promoter and SV40 terminator for Apc2, Apc3, Apc7, Apc8, Apc11 and Apc13 or p10 promoter and HSVtk terminator for Apc1, Apc4, Apc5, Apc6, Apc10, Apc12 and Apc16. TEV cleavable tandem Strep II-tag was fused to Apc6 at C-terminus (Apc6-strep) for affinity purification. Mutant APC/Cs were generated by PCR-based mutagenesis at this step and then all APC/C genes were further cloned into MultiBac vectors creating one pF1 vector-derivative pFUBB carrying Apc3, Apc8 and Apc7 at MUM1 site and Apc5, Apc4 and Apc6-strep at MUM2 site and a second pF1 vector-derivative pFUBB carrying Apc2 and Apc11 at MUM1 site and Apc1 and Apc10 at MUM2 site. A pU1 vector-derivative pUUBB carrying Apc13 at MUM1 site, and Apc12 and Apc16 at MUM2 site was also created. The resultant recombinant transfer vectors were transformed into MultiBacDH10cre cells to generate bacmids by in vivo recombination using the Tn7 sites of the pFUBB vector and the Cre-Lox site of the pUUBB vector. Bacmid 1 incorporated Apc3, Apc8, Apc7, Apc5, Apc4, Apc6-strep, Apc13, Apc12 and Apc16 and Bacmid 2 incorporated Apc2, Apc11, Apc1 and Apc10. Sf9 insect cells were transfected with bacmids 1 and 2 to generate recombinant baculoviruses. To express APC/C complex, High Five insect cells (Invitrogen) at a cell density 1.5 x 10^6 were co-infected with the two recombinant baculoviruses at an MOI (multiplicity of infection) of 1 for each virus and incubated at 27 °C for 48h with shaking (150 rev/min). The cells were harvested, frozen in liquid nitrogen and stored at -80 °C.

Purification of APC/C

All purification steps were performed at 4 °C. Cell pellets were thawed on ice and resuspended in APC/C lysis buffer [50 mM Tris-HCl pH 8.0, 250 mM NaCl, 5% glycerol, 2 mM DTT, 0.5 mM EDTA, 10 µg/ml leupeptin, 10 µg/ml pepstatin A, 10 µg/ml chymostatin, 30 units/ml benzonase (Novagen)] and lysed by sonication. The lysate was centrifuged at 48,400 g for 60 min, the supernatant centrifuged again for 20 min and the final soluble supernatant filtered through a 0.45 µm filter. This cleared lysate was loaded onto a 5 ml Strep-Tactin Superflow Cartridge (Qiagen) at a flow rate of 0.5 ml/min. The column was washed with APC/C wash buffer [50 mM Tris-HCl pH 8.0, 250 mM NaCl, 5% glycerol, 2 mM DTT] at a flow rate of 1.5 ml/min and recombinant APC/C was eluted with APC/C wash buffer containing 2.5 mM desthiobiotin (Sigma). Peak fractions were pooled and concentrated using Amicon Ultra (Millipore), and loaded onto Superose 6 HR 10/30 (GE Healthcare) equilibrated with APC/C SE-D buffer [20 mM Hepes-NaOH pH 7.9, 500 mM NaCl, 2mM DTT, 0.01% n-Dodecyl b-D-maltoside, 10 % glycerol].

Mutant APC/C activity was tested by incubating 1ml lysates with Strep-Tactin Superflow (Qiagen) beads (100 µl) at 4 °C for 1 h, washing with 3 x 1 ml of APC/C wash

buffer and elution with 2 x 300 µl of APC/C wash buffer containing 2.5 mM desthiobiotin. The eluted APC/C proteins were incubated with Dynabeads-Protein A conjugated to anti-Apc3 antibodies (AF3.1) and the bound-APC/C was washed with XB^{CSF} buffer [10mM Hepes-KOH pH7.8, 50mM Sucrose, 100mM KCl, 2mM $MgCl_2$, 5mM EGTA] containing 0.01% NP-40, followed by XB^{CSF} buffer alone. The APC/C bound beads were flash-frozen and stored at -80 °C.

Preparation of *Xenopus* egg cell-free extracts

Meiotic metaphase II-arrested (CSF) *Xenopus laevis* egg extracts were prepared as described (*31*). To prepare interphase extracts, CSF extracts were incubated at 23 °C for 1.5 hr in the presence of 0.4 mM $CaCl_2$ and 10 µg/ml cycloheximide, a protein synthesis inhibitor. Anaphase extracts were prepared by adding nondegradable GST-fused *Xenopus* cyclinBΔ167 (a truncated cyclin B lacking the N-terminal 167 amino acids) to interphase extracts and incubating for 30 min at 23 °C. APC/C depleted (ΔAPC/C) or Cdc20 depleted (ΔCdc20) extracts were prepared as reported previously (*32, 33*). Fresh cycling egg extracts were prepared as described (*34*).

Cell-free destruction and ubiquitylation assays

Destruction assays were performed essentially as described previously (*33*). Substrates were labelled with [^{35}S]methionine (Hartmann Analytic, UK) in a coupled *in vitro* transcription-translation system (Promega, UK) and destruction assays were carried out using *Xenopus* egg cell-free extracts (anaphase or interphase extracts). The samples were taken at the indicated time points and analysed by SDS-PAGE and autoradiography. The images were analysed using Image J (NIH, USA) and the statistical analysis was performed using Prism GraphPad Software (CA, USA). Ubiquitylation assays were essentially performed as described (*35*). Reactions were carried out at 23 °C in 10 µl of buffer (20 mM Tris-HCl pH 7.5, 100 mM KCl, 2.5 mM $MgCl_2$, 2 mM ATP, 0.3 mM DTT) containing 10 ng/µl APC/C, 0.05 mg/ml E1, 0.025 mg/ml UbcX, 0.75 mg/ml ubiquitin, 1 µM ubiquitin-aldehyde, 150 µM MG132, purified His-Cdh1 protein (or Strep-tag Cdc20), and 1 µl of ^{35}S-labeled cyclin B (fission yeast Cdc13). The reactions were stopped at the indicated time points with SDS sample buffer and analysed by SDS-PAGE and autoradiography. To prepare the APC/C phosphorylated by CDK1-cyclin B/p9, the APC/C was incubated in the XB^{CSF} buffer containing 100 µM ATP in the presence of 10 ng/µl human CDK1-cyclin B (a kind gift of Dr. Endicott, Newcastle University, UK) (*36*) and 32 ng/µl *Xenopus* p9 (Cks2) at 23˚C for 40 min. The resultant APC/C was immunoprecipitated and washed by buffer (20 mM Tris-HCl pH7.5, 100 mM KCl, 2.5 mM $MgCl_2$, 0.01% NP-40), and subjected to ubiquitylation.

Phosphorylation assay

For in vitro phosphorylation using purified p9-CDK1-cyclin B, WT or mutant recombinant APC/Cs bound to Dynabeads-Protein A conjugated to anti-Apc3 antibodies (AF3.1) were incubated in the XB^{CSF} buffer containing 100 µM cold ATP and 1 µCi/nmol of [γ-^{32}P] ATP (Hartmann Analytic, UK) in the presence of 10 ng/µl human CDK1-cyclin B (*36*) and 32 ng/µl *Xenopus* p9 (Cks2) at 23˚C for 20 min or 40 min. For phosphorylation assay in *Xenopus* egg extracts, the APC/C was incubated with APC/C-depleted egg extract in the presence of [γ-^{32}P] ATP and cyclinBΔ167 at 23˚C for 45 min.

The APC/C was immuno-precipitated and boiled in SDS sample buffer and analysed by SDS-PAGE and autoradiography.

Immunoprecipitation of APC/C

The APC/C was immunoprecipitated using Apc3 MAb (AF3.1) immobilized Dynabeads protein A. The bound proteins were washed twice with XB^{CSF_HS} [XB^{CSF} containing 500 mM KCl and 0.01% NP-40], eluted with SDS sample buffer and analysed by SDS-PAGE and immunoblotting.

Cloning and purification of *Xenopus* Apc1 fragments

The fragment (294-399) of *Xenopus tropicalis* Apc1 was fused to 3xFlag tag at N-terminus and 6xHis tag at C-terminus, and subcloned into pET vector. Mutants were generated by PCR-based mutagenesis. The resultant plasmids were introduced into BL21-CodonPlus (DE3) and the fusion proteins were expressed at 37 °C for 1hr in the presence of 1 mM IPTG. The cells were lysed by 0.3 mg/ml lysozyme, sonicated in lysis buffer [20 mM Hepes-NaOH pH 7.9, 500 mM NaCl, 5mM EGTA, 10 μg/ml leupeptin, 10 μg/ml pepstatin A, 10 μg/ml chymostatin, 0.1 % Triton X-100, 10mM imidazole]. The proteins were purified from clarified lysate on Ni-NTA agarose beads (Qiagen).

Binding assay using *Xenopus* Apc1 fragments

Purified Apc1 fragments were incubated with Anti-Flag Affinity M2 beads (Sigma) at 4 °C for 0.5-1h. Beads were washed with XB^{CSF} buffer and incubated with interphase extract in the presence or absence of cyclin BΔ167 at 23 °C for 45 min, separated from extract on Micro Bio-Spin columns (Bio-Rad), and washed twice with XB^{CSF} buffer containing 0.1% NP-40. The bound proteins were eluted with SDS-sample buffer and analysed by SDS-PAGE and immunoblotting.

Antibodies

Antibodies used are as follows: anti-Apc1 (RbAb 4853, 1:100), Apc2 (RbAb 7577, 1:500), Apc3/Cdc27 (1:200; BD Transduction Laboratories), Apc5 (RbAb 3445, 1:500), Apc6 (RbAb 3446, 1:500), Cdc20 (MAb BA8, 1:100), Xe-p9 (RbAb CE/R2, 1:50), phospho-Plx1 (MAb AZ44, 1:1000), Cdc2 (MAb A17, 1:3000). Apc1 phosphopeptide antibody (anti-pS314pS318, 1:1000) was raised in rabbits against LPH (the horseshoe crab *Limulus polyphemus* hemocyanin) conjugated phosphopeptide CVSKGEpSPTApSPFQN (BioGenes, Germany). Antibodies were affinity purified using a phosphopeptide column prepared with SulfoLink Kit (Pierce). After elution with ImmunoPure Gentle Ag/Ab Elution Buffer (Pierce), antibodies were dialysed against TBS and non-phosphospecific antibody was affinity depleted by passing through a column cross-linked with non-phosphopeptide CVSKGESPTASPFQN. The eluted phospho-specific antibodies were then enriched by dialysis against TBS containing 50% glycerol.

Author Contributions

K.F and H.Y. designed and performed the experiments, analysed and interpreted data, and wrote the manuscript. M.G. contributed towards the cloning and expression of recombinant APC/C. H.Y. conceived and supervised the overall research.

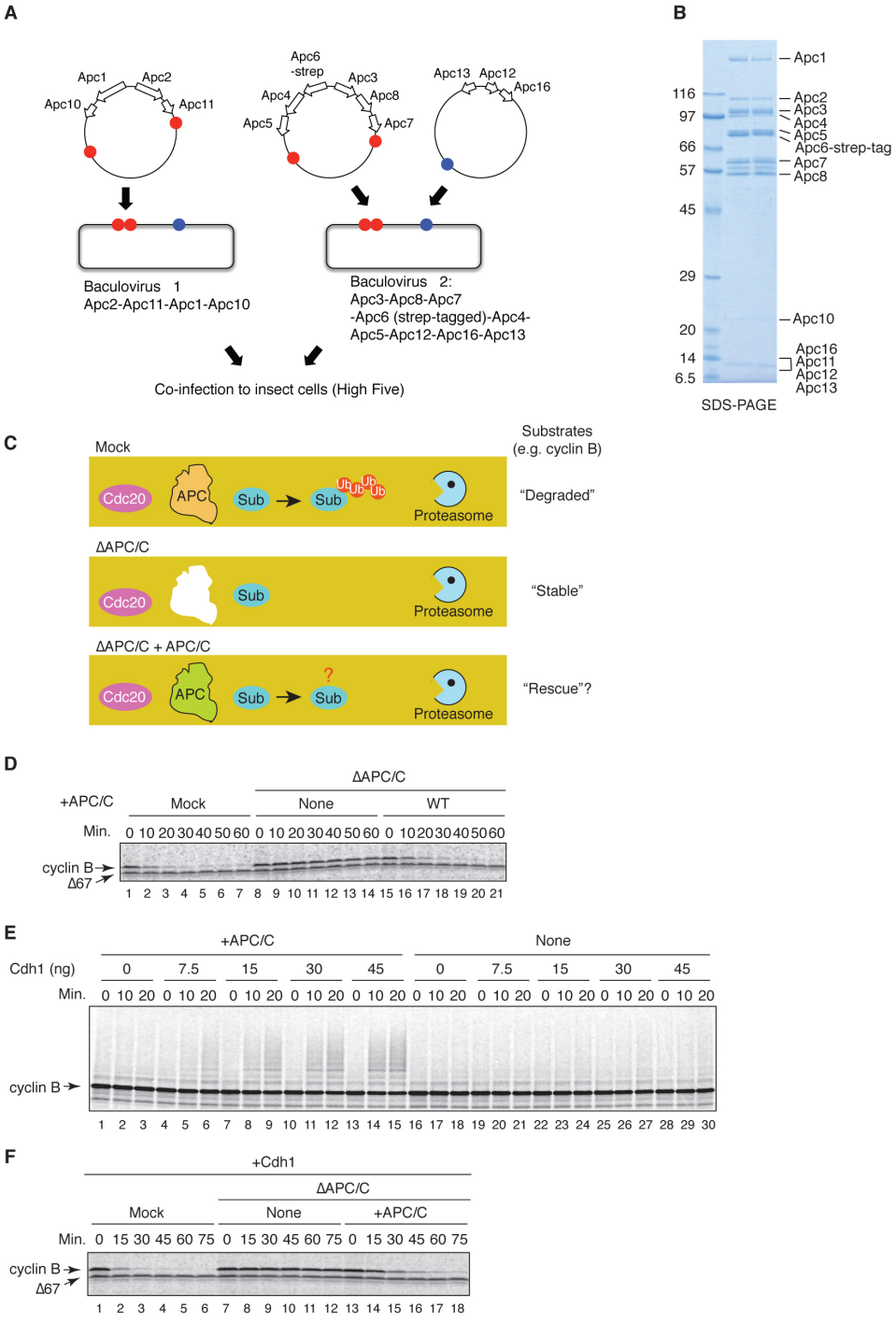

Fig.S1.
Multi-subunit APC/C reconstitution and cell-free APC/C functional assays.
(A) Schematic illustration of the expression of recombinant *Xenopus* apo-APC/C (APC/C). APC/C subunit genes were cloned into plasmid, and transferred into bacmid by recombination as shown. Red and blue circles are Tn7 transposition site and Cre-LoxP sites, respectively. The resultant two baculoviruses were used to co-infect High Five

insect cells and the APC/C was purified by affinity chromatography using Strept-Tactin resin. **(B)** Reconstituted WT APC/C was bound to a Strept-Tactin column, eluted by desthiobiotin, concentrated and applied to a Superose 6 column. The peak fraction was run on SDS-PAGE gradient gel, and stained with Coomassie Brilliant Blue (CBB). The CBB staining pattern confirms the high-purity and quality of expression of APC/C. **(C)** *Xenopus* egg cell-free extract based APC/C functional assay. APC/C substrates such as cyclin B can be degraded in *Xenopus* egg extract but if endogenous APC/C is depleted (ΔAPC/C), cyclin B becomes stable. Reconstituted APC/Cs that contain mutation(s) in any subunit(s) can be created and their activity tested in ΔAPC/C extracts (ΔAPC/C+APC/C). **(D)** Reconstituted WT APC/C supports cyclin B destruction. Cdc20-dependent cyclin destruction assay in *Xenopus* egg cell-free extracts. Mock or WT APC/C was incubated in ΔAPC/C anaphase extract. ^{35}S-labelled cyclin B and a version of cyclin B lacking the N-terminal 67 residues (Δ67, stable control) were used as substrates. Samples taken at indicated time points after addition of substrates were analysed by SDS–PAGE and autoradiography. A lack of cyclin destruction in ΔAPC/C anaphase extract was restored by adding back WT APC/C (lanes 15-21). **(E)** Reconstituted WT APC/C is a functional ubiquitin ligase. WT APC/C (lanes 1-15) or none (lanes 16-30) was incubated with ubiquitylation factors (E1, E2, energy generating mix, ubiquitin) at 23°C. ^{35}S-labelled cyclin B (fission yeast Cdc13) and purified Cdh1 were used as substrate and co-activator, respectively. Samples taken at indicated time points were analysed by SDS–PAGE and autoradiography. **(F)** Cdh1 can activate APC/C in interphase and trigger cyclin B destruction (lanes 1-6). Mock or WT APC/C was incubated in ΔAPC/C interphase extract supplemented with Cdh1 (lanes 7-18). Please note that *Xenopus* eggs and early embryos lack Cdh1 until MBT (midblastula transition). ^{35}S-labelled cyclin B and a version of cyclin B lacking the N-terminal 67 residues (Δ67, stable control) were used as substrates. A lack of cyclin destruction in ΔAPC/C interphase extract was restored by adding back WT APC/C (lanes 13-18).

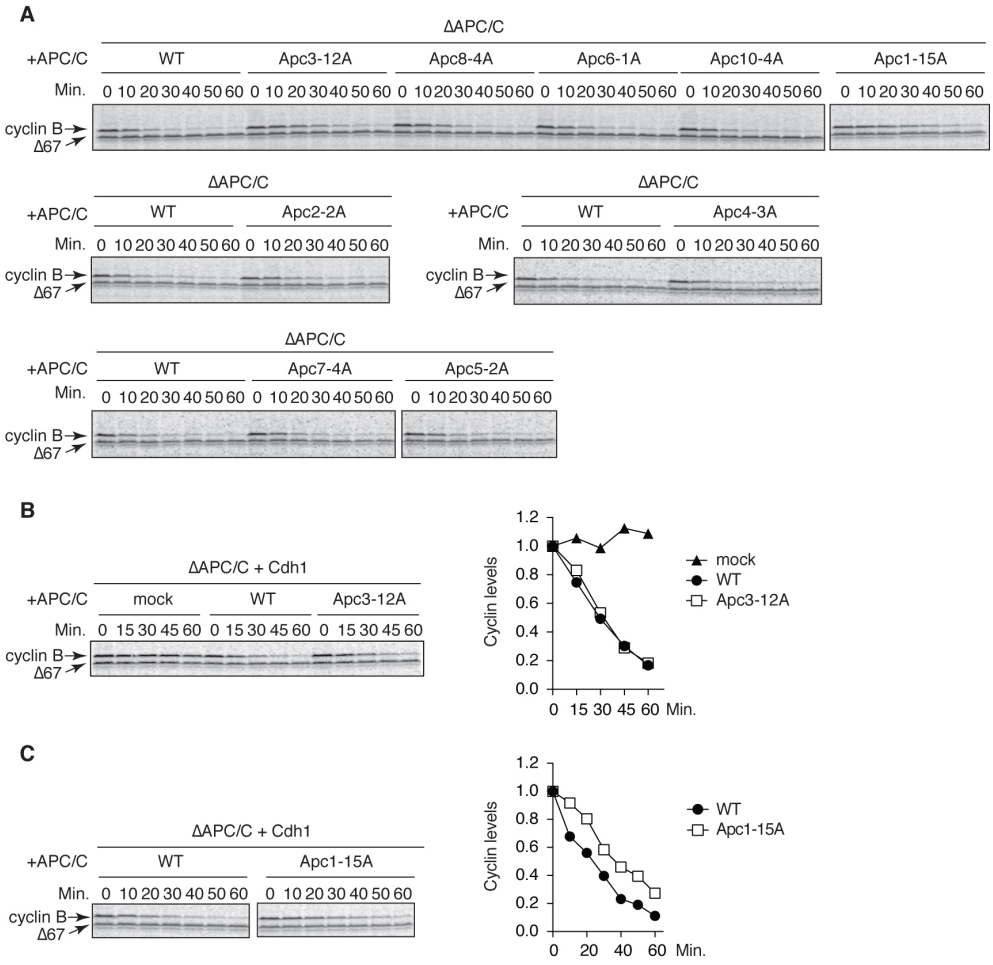

Fig. S2.

A screening of APC/Cs harbouring CDK site mutations. (A) Cyclin destruction assay in *Xenopus* egg cell-free extracts. Mock or endogenous APC/C-depleted anaphase extracts (ΔAPC/C) were supplemented with a range of reconstituted APC/Cs (table S1). ^{35}S-labelled cyclin B and a version of cyclin B lacking the N-terminal 67 residues (Δ67, stable control) were used as substrates. Samples taken at indicated time points after addition of substrates were analysed by SDS–PAGE and autoradiography. Quantification of the destruction assays is shown in Fig. 1A. **(B)** The activity of APC/C$^{3\text{-}12A}$ in interphase. Left panel: Mock, APC/C^{WT} or APC/C$^{3\text{-}12A}$ mutant complex was incubated in APC/C-depleted (ΔAPC/C) interphase extract supplemented with Cdh1 and ^{35}S-labelled APC/C substrates (cyclin B and Δ67). Samples taken at indicated time points after addition of substrates were analysed by SDS–PAGE and autoradiography. Right panel: Quantification of Left panel. Relative levels of cyclin B are shown. **(C)** The activity of APC/C$^{1\text{-}15A}$ in interphase. Same as **(B)**, but APC/C^{WT} or APC/C$^{1\text{-}15A}$ mutant complex was used.

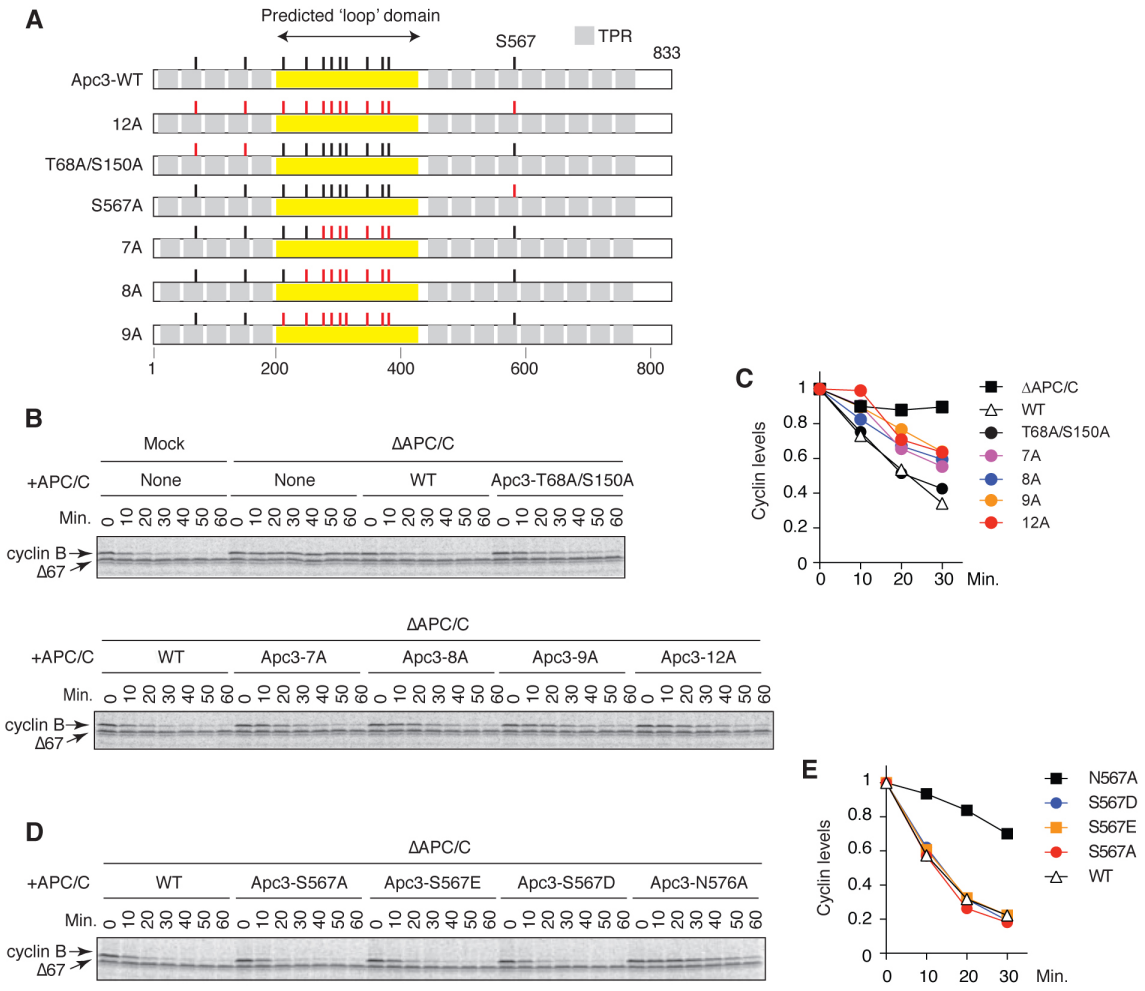

Fig. S3

The activities of a series of mutant APC/Cs carrying mutations in Apc3 in *Xenopus* egg anaphase extracts. (A) Schematic diagram of Apc3 and its phosphorylation site mutants. SP/TP sites shared between *Xenopus* and Human Apc3 are shown in black, mutated sites in red. (**B**) The activities of the indicated Apc3 mutant APC/Cs were assessed using cyclin destruction assay, like fig. S2A. **(C)** Quantification of the destruction assays (**B**). **(D)** The impact of S567 phosphorylation on APC activity was carefully investigated as S567 is located close to the IR-binding domain. WT or APC/Cs carrying S567 mutation (substitution to alanine, aspartic acid or glutamic acid) in the TPR domain (Apc3-S567A, Apc3-S567D, Apc3-S567E) were examined. The N576A mutant was used as a control because this residue is highly conserved among species and is known to be important for APC/C activity (*19*). **(E)** Quantification of the destruction assays (**D**).

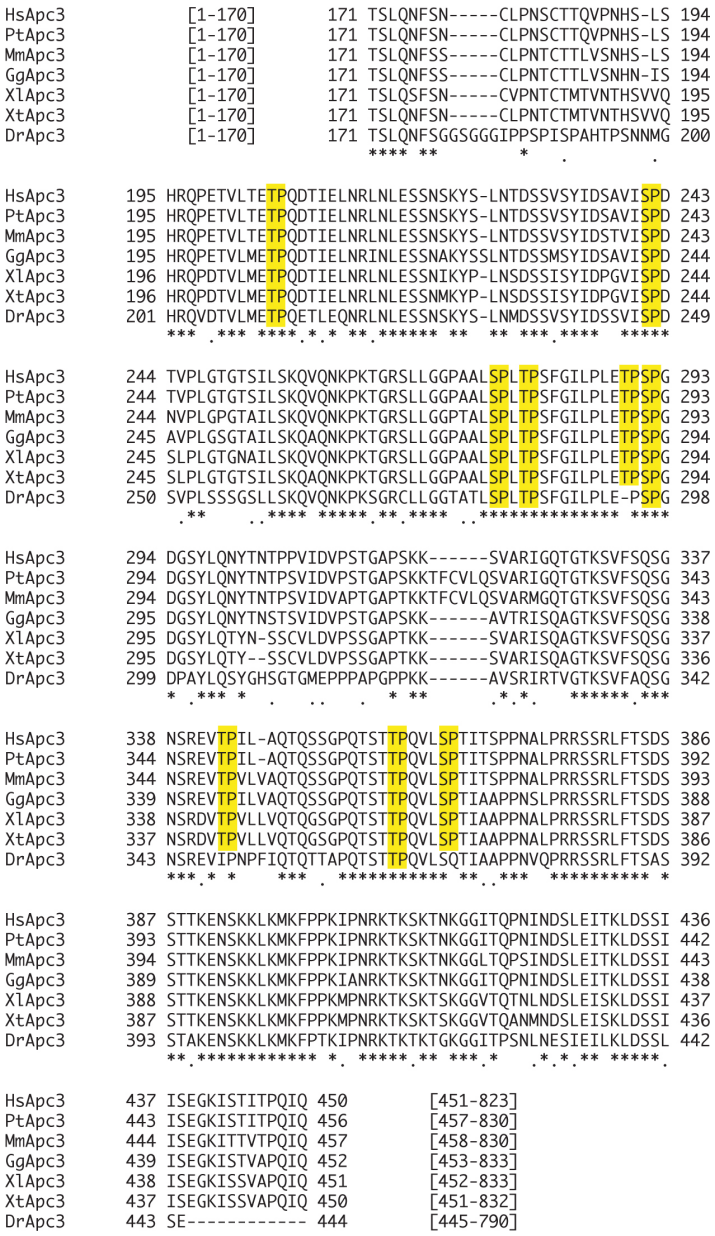

Fig. S4.

Alignment of predicted loop domains of vertebrate Apc3. Conserved CDK consensus phosphorylation sites (SP/TP) in a predicted Apc3 loop among vertebrates are highlighted in yellow (Hs; *Homo sapiens* human, Pt; *Pan troglodytes* chimpanzee, Mm; *Mus musculus* mouse, Gg; *Gallus gallus* chicken, Xl; *Xenopus laevis* frog, Xt; *Xenopus tropicalis* frog, Dr; *Danio rerio* zebrafish).

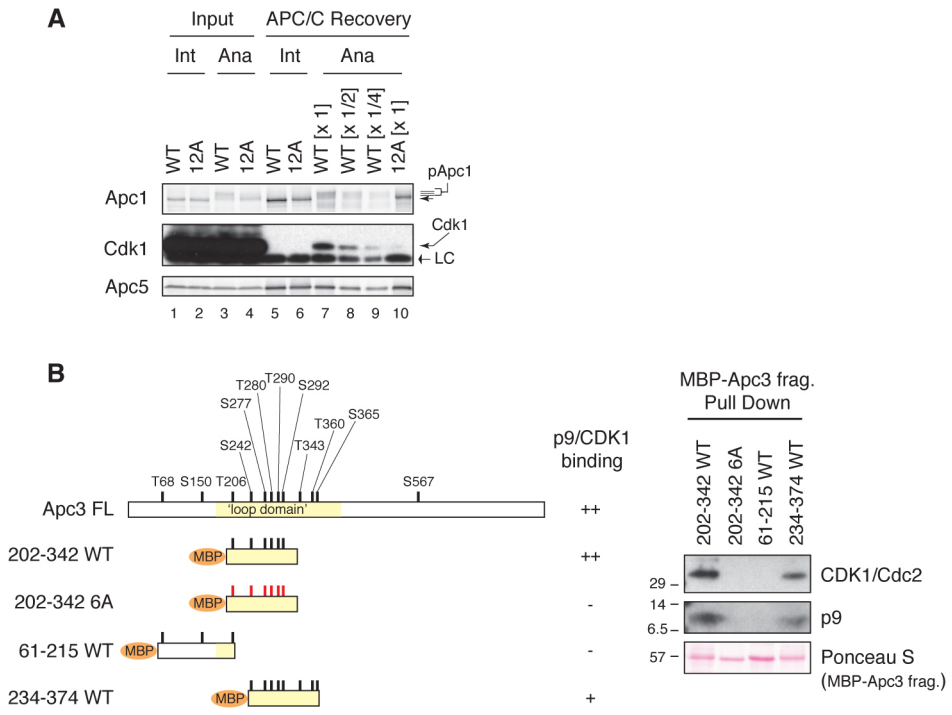

Fig. S5.

The loop domain of Apc3 binds p9-CDK1 in a phosphorylation-dependent manner. **(A)** WT APC/C or APC/C$^{Apc3\text{-}12A}$ was incubated with ΔAPC/C interphase or anaphase extracts. The APC/C was recovered with anti-Apc3 beads and bound proteins were analysed by immunoblotting. Different volumes of APC/Cs were loaded to quantitatively examine levels of Cdk1 associated and Apc1 phosphorylation on APC/C$^{Apc3\text{-}12A}$, compared with WT APC/C. LC; IgG light chain. **(B)** Left panel: Schematic diagram of Apc3 fragments used. Right panel: Bacterially purified MBP-tagged Apc3 fragments were incubated with *Xenopus* egg CSF-arrested extracts for 20 min and Apc3 bound proteins were analysed by SDS–PAGE and immunoblotting. The loop domain fragment (residues 202-342) binds p9 in mitotic egg extracts, whereas the same fragment with CDK mutations (residues 202-342 6A) abolishes p9-binding activity. A similar length fragment from the N-terminal domain (residues 61-215) does not bind whereas a second fragment (residues 234-374) containing the loop domain is able to bind to p9 and CDK1, albeit with a weaker interaction than the loop domain fragment (residues 202-342).

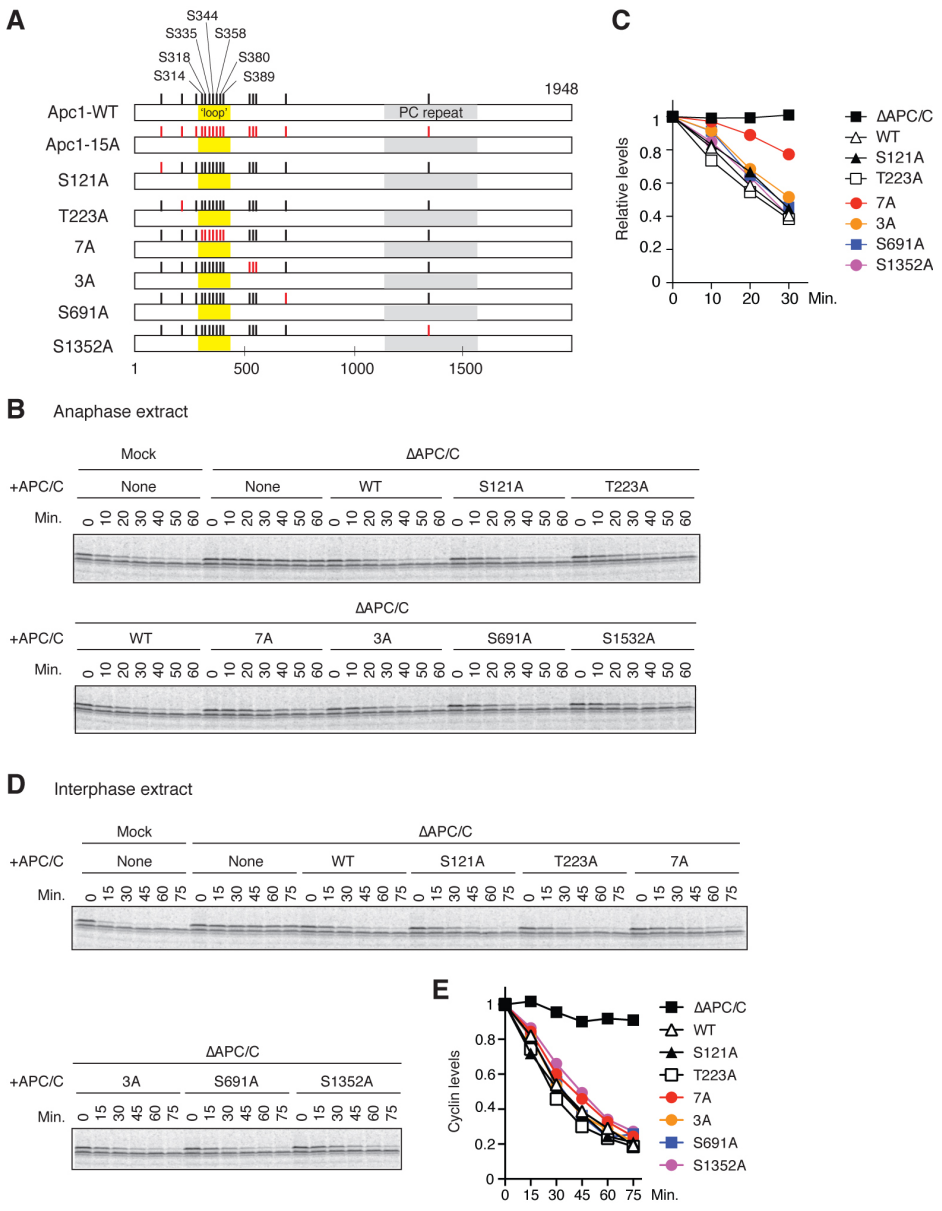

Fig. S6.

The activities of a series of mutant APC/Cs carrying mutations in Apc1 in *Xenopus* egg extracts. (A) Schematic diagram of Apc1 and its phosphorylation site mutants used. SP/TP sites shared between *Xenopus* and Human Apc1 are shown in black, mutated sites in red. **(B)** Cyclin destruction assay in anaphase extracts. The indicated mutant APC/C were incubated with ΔAPC/C anaphase extracts and then substrates ^{35}S-labelled cyclin B and Δ67 (as a stable control) were added. Samples taken at indicated time points after addition of substrates, were analysed by SDS–PAGE and autoradiography. **(C)** Quantification of the destruction assays **(B)**. **(D)** Cyclin destruction assay in interphase extracts. Using the same APC/Cs as **(B)**, the activities of indicated mutant APC/Cs were assessed by destruction assay in APC/C-depleted (ΔAPC/C) interphase extract supplemented with Cdh1 and ^{35}S-labelled APC/C substrates (cyclin B and Δ67). Samples

taken at indicated time points after addition of substrates were analysed by SDS–PAGE and autoradiography. **(E)** Quantification of the destruction assays **(D)**.

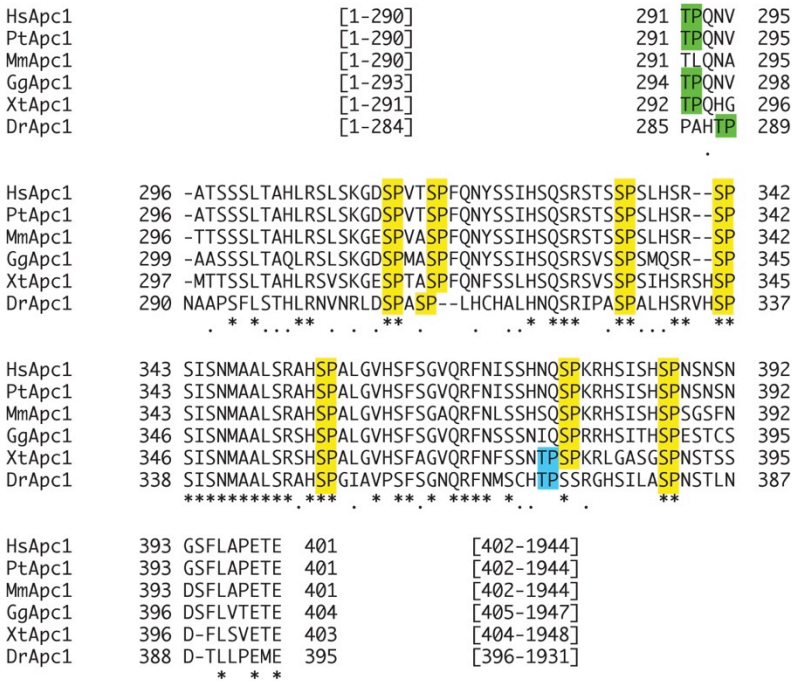

Fig. S7.

Alignment of predicted loop domains of vertebrate Apc1. Conserved CDK consensus phosphorylation sites (SP/TP) in a predicted Apc1 loop among vertebrates are highlighted (Hs; *Homo sapiens* human, Pt; *Pan troglodytes* chimpanzee, Mm; *Mus musculus* mouse, Gg; *Gallus gallus* chicken, Xt; *Xenopus tropicalis* frog, Dr; *Danio rerio* zebrafish). Highly conserved (Yellow), Conserved apart from *Mus musculus* (Green), Conserved between *Xenopus tropicalis* and *Danio rerio* (Blue)

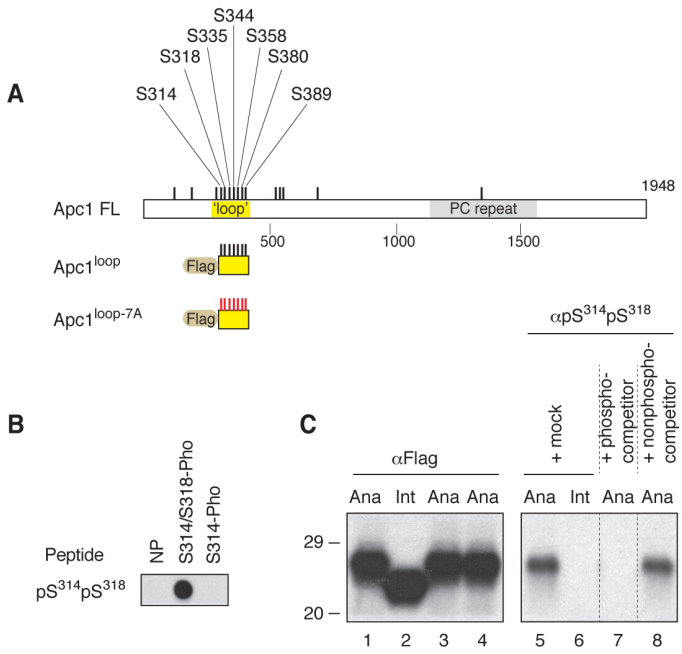

Fig. S8.

The specificity of phospho-specific Apc1 antibody. (A) Schematic diagram of Apc1 full length (FL) and its flexible loop domain fragments (residues 294-399): Apc1^{loop} and Apc1$^{loop\text{-}7A}$. The mutated CDK sites are in red. **(B)** Antibody binding to synthetic Apc1 peptides with no phosphorylation (NP), phosphorylation at S314 and S318 (S314/S318-Pho) or single site phosphorylation at S314 (S314-Pho). Peptides were spotted onto a nitrocellulose membrane and blotted with phospho-S314-S318 antibody (pS314pS318). **(C)** The pS314pS318 antibody specifically recognises Apc1 only when they are phosphorylated in anaphase. Bacterially purified Flag-tagged WT Apc1^{loop} fragment was incubated in anaphase or interphase extracts for 45 min, purified using anti-FLAG affinity beads and analysed by immunoblotting with anti-Flag (Left: lanes 1-4) or anti-pS314pS318 (Right: lanes 5-8) antibodies. An excess of the corresponding epitope phospho-peptide (lane 7) or the same non-phosphorylated peptide (lane 8: nonphospho-peptide competitor) was incubated with the pS314pS318 antibody during immunoblotting. The pS314pS318 antibody recognises Apc1^{loop} only when it is phosphorylated in anaphase (lanes 5 and 6) and the band disappears if the antibody is neutralized by the blocking peptide (lane 7).

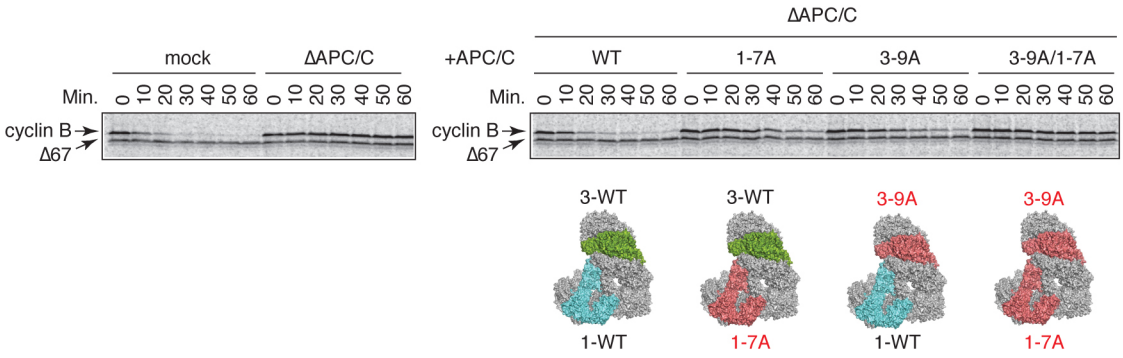

Fig. S9.
Phosphorylation of Apc1 and Apc3 subunits is crucial for APC/C activation.
Upper panel: Cyclin destruction assay in mock or ΔAPC/C anaphase extract or ΔAPC/C anaphase extract supplemented with WT, Apc1-7A, Apc3-9A single or Apc3-9A/Apc1-7A double mutant APC/Cs. ^{35}S-labelled cyclin B and cyclin B lacking the N-terminal 67 residues (Δ67, stable control) were used as substrates. Samples taken at indicated time points after addition of substrates were analysed by SDS–PAGE and autoradiography. Quantification of the destruction assays is shown in Fig. 3A. Lower panel: 3D images of the APC/C showing WT Apc1 (cyan), Apc3 (green) and mutated subunits in red.

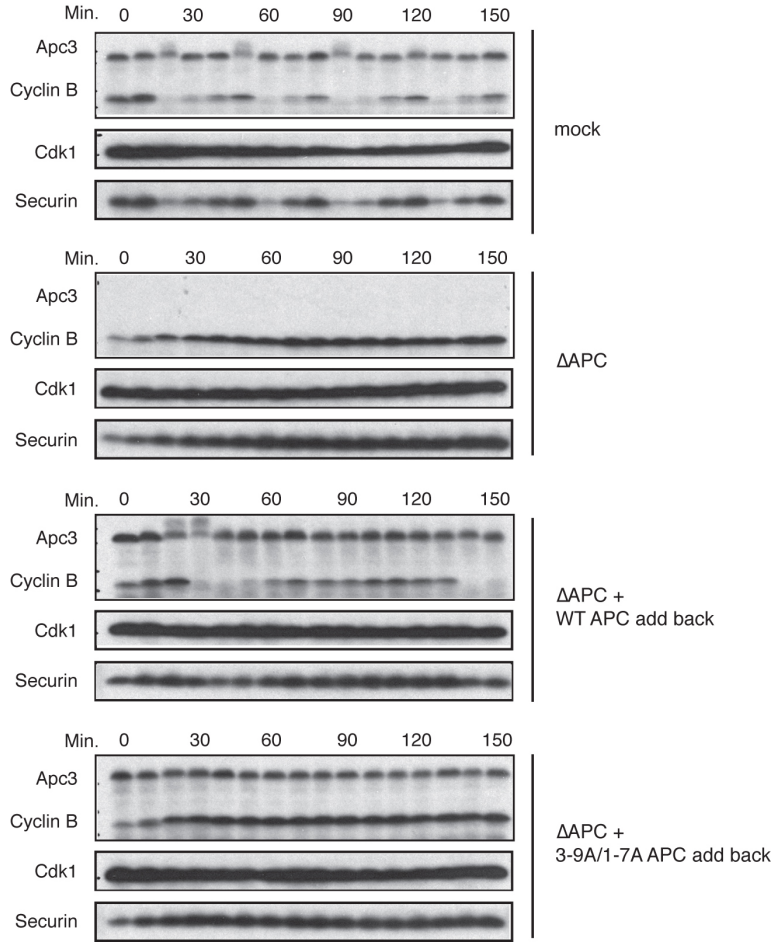

Fig. S10.
The APC/C$^{Apc3\text{-}9A/Apc1\text{-}7A}$ is inactive and unable to support cyclin B or securin proteolysis. Fresh "cycling" frog extracts and endogenous APC/C-depleted cycling extracts (ΔAPC) were prepared. WT or Apc3-9A/Apc1-7A double mutant APC/C (3-9A/1-7A) was added back to ΔAPC extracts. Egg extracts were incubated at 23˚C and samples were taken every 10 min for analysis. Apc3, cyclin B2, Cdk1 and securin were detected by immunoblotting. The control (mock) cycling extracts performed cycles of entry into and exit from mitosis, judging from band shifts of Apc3 and disappearance of cyclin B and securin whereas ΔAPC never degraded cyclin B nor securin. WT APC/C, but not APC/C$^{Apc3\text{-}9A/Apc1\text{-}7A}$ rescued ΔAPC extracts, allowing cyclin B and securin destruction.

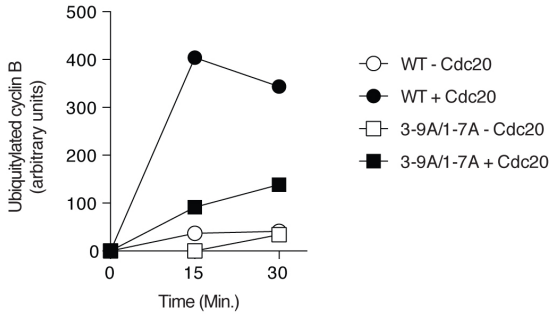

Fig. S11.
In vitro phosphorylated APC/C$^{Apc3\text{-}9A/Apc1\text{-}7A}$ is less active than APC/C^{WT} in the presence of Cdc20. Quantification of the ubiquitylation assays (Fig. 3C).

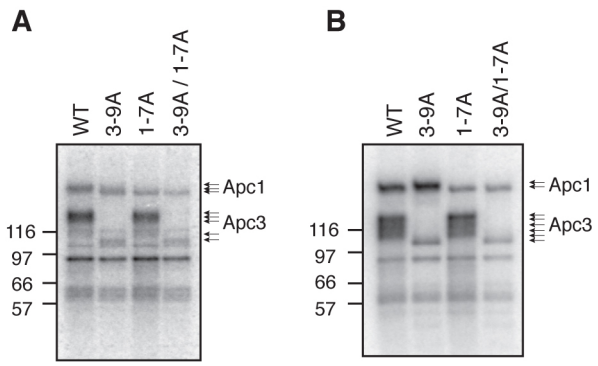

Fig. S12.

Phosphorylation status of WT or CDK site mutant APC/Cs in anaphase egg extract and during in vitro phosphorylation by CDK-cyclin B. (A) WT APC/C, APC/$C^{Apc3\text{-}9A}$, APC/$C^{Apc1\text{-}7A}$ or APC/$C^{Apc3\text{-}9A/Apc1\text{-}7A}$ was incubated in ΔAPC egg extract in the presence of [γ-^{32}P] ATP and cyclinBΔ167 at 23 ˚C for 45 min ('anaphase' extract). The APC/C was recovered using anti-Apc3 affinity beads as Fig. 1B and phosphorylation of APC/Cs was analysed by SDS-PAGE and autoradiography. The phosphorylation levels of Apc3-9A and Apc1-7A mutant APC/Cs were decreased, compared with WT. Note that both Apc3-9A and Apc1-7A still contain CDK phosphorylation sites located in the non-loop domain and also under these conditions add-back APC/C can be phosphorylated by any mitotic kinases in *Xenopus* egg extracts. In anaphase extract, phosphorylation of Apc1 is reduced if phosphorylation of Apc3 is blocked (see also Fig. 2E). **(B)** WT APC/C, APC/$C^{Apc3\text{-}9A}$, APC/$C^{Apc1\text{-}7A}$ or APC/$C^{Apc3\text{-}9A/Apc1\text{-}7A}$ was incubated with CDK1-cyclin B and p9 in the presence of [γ-^{32}P] ATP at 23˚C for 40 min. The APC/C was recovered using anti-Apc3 affinity beads, and analysed by SDS-PAGE and autoradiography. In purified p9-CDK1-cyclin B-dependent assay, phosphorylation of Apc1 is observed even if phosphorylation of Apc3 is blocked. The mechanism behind the difference between egg extracts and the purified CDK system remains unknown.

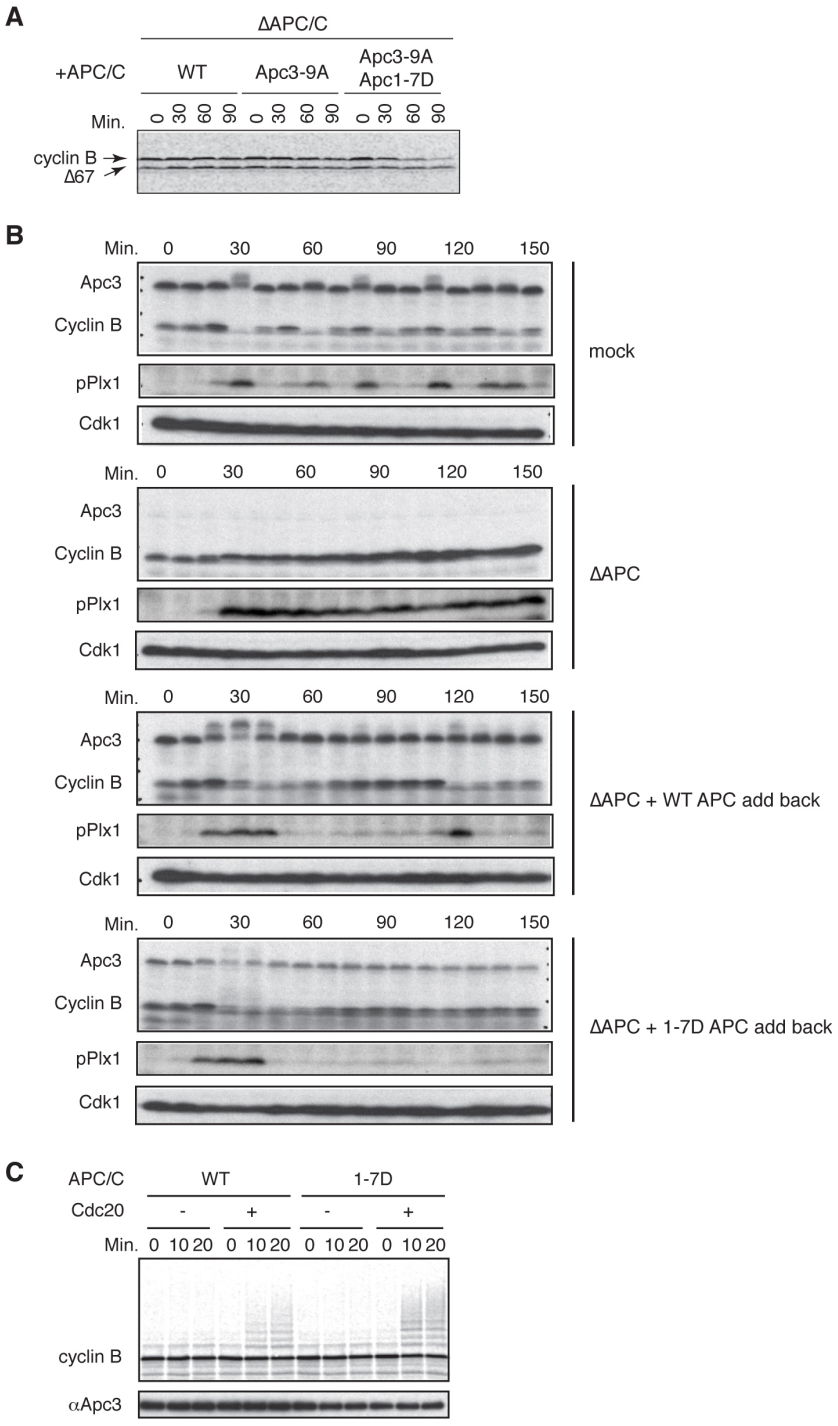

Fig. S13.
The APC/C$^{Apc1\text{-}7D}$ is more active than WT APC/C in interphase.
(A) Cyclin destruction assay in interphase extracts. WT APC/C, APC/C$^{Apc3\text{-}9A}$ or APC/C$^{Apc3\text{-}9A/Apc1\text{-}7D}$ was incubated with ΔAPC/C interphase extract and samples taken at indicated time points after addition of substrates were analysed by SDS–PAGE and autoradiography. Quantification of the destruction assays is shown in Fig. 3D. (**B**)

Endogenous APC/C was immunodepleted from fresh cycling extract (ΔAPC) and either WT or Apc1-7D mutant APC/C added back. Egg extracts were incubated at 23˚C and samples were taken every 10 min for analysis. Apc3, cyclin B2, phosphorylated Plx1 (pPlx1:AZ44) and Cdk1 were detected by immunoblotting. As controls, mock and ΔAPC extracts are shown. In the presence of APC/C$^{Apc1\text{-}7D}$, cyclin B does not sufficiently accumulate after the first mitotic exit (see between 60 min and 110 min) compared with WT APC add back and thus fails to enter the second mitosis which occurs at 120 min with WT APC/C. **C)** Unphosphorylated WT APC/C or APC/C$^{Apc1\text{-}7D}$ was incubated with ubiquitylation factors (E1, E2, energy generating mix, ubiquitin) in the presence/absence of Cdc20 at 23°C. ^{35}S-labelled cyclin B (fission yeast Cdc13) was used as substrate. Samples taken at indicated time points were analysed by SDS–PAGE and autoradiography. The amounts of APC/C used were monitored by anti-Apc3 immunoblotting.

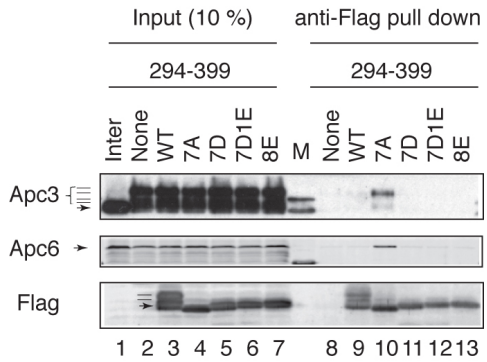

Fig. S14.

Apc1^{loop} binds to the APC/C depending on its phosphorylation status. Phospho-mimetic mutation into Apc1^{loop} abolishes the ability to interact with APC/C. Seven CDK sites in Flag-tagged Apc1 loop fragment were substituted to alanine, aspartic acid or glutamic acid with an additional mutation in 7D1E and 8E (T378E). Wild type Apc1 fragment (WT) or its derivatives carrying mutations in CDK sites (7A, 7D, 7D1E or 8E) was incubated in anaphase extract and immunopurified with anti-FLAG affinity beads. Bound proteins were analysed by immunoblotting. M; molecular marker, staining pattern is a result of crossreaction with anti-Apc3 and anti-Apc6 antibodies.

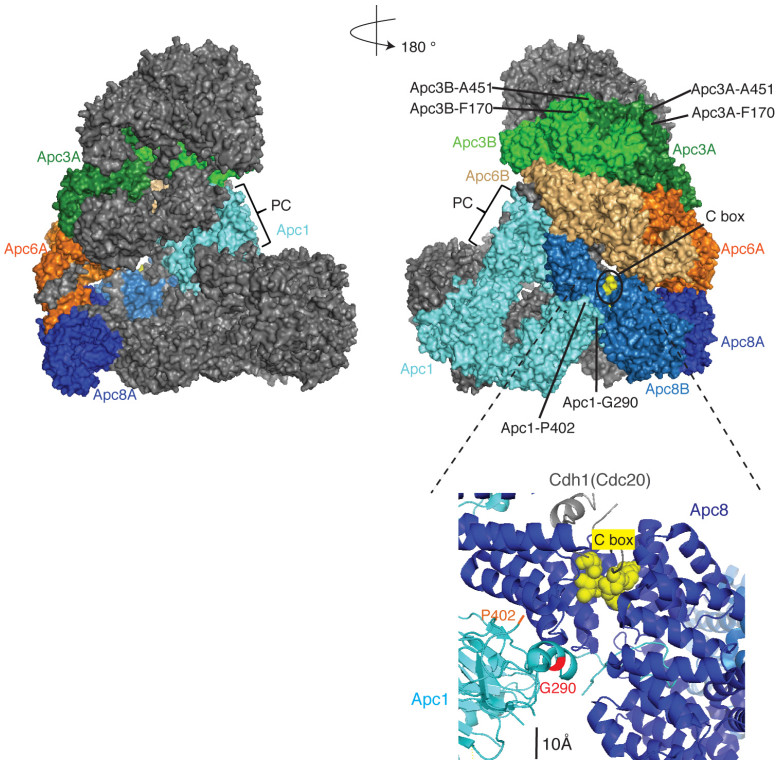

Fig. S15.

Location of Apc1, Apc3, Apc6, Apc8 and C box in human APC/C-Cdh1-Emi1 complex. Top: The image was generated using the Protein Data Bank file (4UI9: APC/C$^{Cdh1.Emi1}$)(*25*) and PyMOL, highlighting Apc1 (cyan), Apc3A (green), Apc3B (light green), Apc6A (orange), Apc6B (light orange), Apc8A (blue), Apc8B (light blue) and the C box region (SKHGDRFIPSRAG, yellow). The PC domain of Apc1 (PC) and the N- and C- terminal residues of predicted loop domains of Apc1 and Apc3 are indicated. Note that each of Apc3, Apc6 and Apc8 forms symmetric V-shaped homo-dimers through their N-terminal regions. Bottom: Closed view of the interaction interface of three subunits, Apc1, Apc8 and the C-box from Cdh1/Cdc20. The location of Apc1^{loop} is not determined, but the assigned adjacent sites such as G290 (red) and P402 (orange) in Apc1 are very close to the interface between the C-box (yellow) and Apc8.

Table S1. CDK phosphorylation site mutant APC/C

APC/C subunit	No. of conserved CDK sites (SP/TP)	APC/C mutant	CDK mutation sites
APC1	15	Apc1-15A	S121A, T223A, T292A, S314A, S318A, S335A, S344A, S358A, S380A, S389A, T532A, T539A, S558A, S691A, S1352A
APC2	2	Apc2-2A	T303A, S648A
APC3	12	Apc3-12A	T68A, S150A, T206A, S242A, S277A, T280A, T290A, S292A, T343A, T360A, S365A, S567A
APC4	3	Apc4-3A	S22A, S481A, S503A
APC5	2	Apc5-2A	T31A, T235A
APC6	1	Apc6-1A	S558A
APC7	4	Apc7-4A	S38A, T92A, T134A, S523A
APC8	4	Apc8-4A	S544A, T565A, S571A, T579A
APC10	4	Apc10-4A	T3A, T7A, T90A, T160A
APC11	0		
APC12	0		
APC13	0		
APC16	1		

References and Notes

1. V. Sudakin *et al.*, The cyclosome, a large complex containing cyclin-selective ubiquitin ligase activity, targets cyclins for destruction at the end of mitosis. *Mol Biol Cell* **6**, 185-197 (1995).
2. S. Irniger, S. Piatti, C. Michaelis, K. Nasmyth, Genes involved in sister chromatid separation are needed for B-type cyclin proteolysis in budding yeast. *Cell* **81**, 269-278 (1995).
3. R. W. King *et al.*, A 20S complex containing CDC27 and CDC16 catalyzes the mitosis-specific conjugation of ubiquitin to cyclin B. *Cell* **81**, 279-288 (1995).
4. I. Primorac, A. Musacchio, Panta rhei: The APC/C at steady state. *J Cell Biol* **201**, 177-189 (2013).
5. L. Chang, D. Barford, Insights into the anaphase-promoting complex: a molecular machine that regulates mitosis. *Current opinion in structural biology* **29C**, 1-9 (2014).
6. J. Pines, Cubism and the cell cycle: the many faces of the APC/C. *Nat Rev Mol Cell Biol* **12**, 427-438 (2011).
7. H. C. Huang, J. Shi, J. D. Orth, T. J. Mitchison, Evidence that mitotic exit is a better cancer therapeutic target than spindle assembly. *Cancer Cell* **16**, 347-358 (2009).
8. E. Manchado *et al.*, Targeting mitotic exit leads to tumor regression in vivo: Modulation by Cdk1, Mastl, and the PP2A/B55alpha,delta phosphatase. *Cancer Cell* **18**, 641-654 (2010).
9. X. Zeng *et al.*, Pharmacologic inhibition of the anaphase-promoting complex induces a spindle checkpoint-dependent mitotic arrest in the absence of spindle damage. *Cancer Cell* **18**, 382-395 (2010).
10. K. L. Sackton *et al.*, Synergistic blockade of mitotic exit by two chemical inhibitors of the APC/C. *Nature* **514**, 646-649 (2014).
11. K. E. Gascoigne, S. S. Taylor, Cancer cells display profound intra- and interline variation following prolonged exposure to antimitotic drugs. *Cancer Cell* **14**, 111-122 (2008).
12. J. A. Steen *et al.*, Different phosphorylation states of the anaphase promoting complex in response to antimitotic drugs: a quantitative proteomic analysis. *Proceedings of the National Academy of Sciences of the United States of America* **105**, 6069-6074 (2008).
13. C. Kraft *et al.*, Mitotic regulation of the human anaphase-promoting complex by phosphorylation. *EMBO J* **22**, 6598-6609 (2003).
14. E. R. Kramer, N. Scheuringer, A. V. Podtelejnikov, M. Mann, J. M. Peters, Mitotic regulation of the APC activator proteins CDC20 and CDH1. *Mol Biol Cell* **11**, 1555-1569 (2000).
15. M. Shteinberg, A. Hershko, Role of Suc1 in the activation of the cyclosome by protein kinase Cdk1/cyclin B. *Biochem Biophys Res Commun* **257**, 12-18 (1999).
16. G. Fang, H. Yu, M. W. Kirschner, Direct binding of CDC20 protein family members activates the anaphase-promoting complex in mitosis and G1. *Mol Cell* **2**, 163-171 (1998).

17. Z. Zhang *et al.*, Recombinant expression, reconstitution and structure of human anaphase-promoting complex (APC/C). *Biochem J* **449**, 365-371 (2013).
18. I. Berger, D. J. Fitzgerald, T. J. Richmond, Baculovirus expression system for heterologous multiprotein complexes. *Nat Biotechnol* **22**, 1583-1587 (2004).
19. M. E. Matyskiela, D. O. Morgan, Analysis of activator-binding sites on the APC/C supports a cooperative substrate-binding mechanism. *Mol Cell* **34**, 68-80 (2009).
20. D. Patra, W. G. Dunphy, Xe-p9, a Xenopus Suc1/Cks homolog, has multiple essential roles in cell cycle control. *Genes & development* **10**, 1503-1515 (1996).
21. D. Patra, W. G. Dunphy, Xe-p9, a Xenopus Suc1/Cks protein, is essential for the Cdc2-dependent phosphorylation of the anaphase- promoting complex at mitosis. *Genes & development* **12**, 2549-2559 (1998).
22. A. D. Rudner, A. W. Murray, Phosphorylation by Cdc28 activates the Cdc20-dependent activity of the anaphase-promoting complex. *J Cell Biol* **149**, 1377-1390 (2000).
23. M. Koivomagi *et al.*, Multisite phosphorylation networks as signal processors for Cdk1. *Nature structural & molecular biology* **20**, 1415-1424 (2013).
24. D. A. McGrath *et al.*, Cks confers specificity to phosphorylation-dependent CDK signaling pathways. *Nature structural & molecular biology* **20**, 1407-1414 (2013).
25. L. Chang, Z. Zhang, J. Yang, S. H. McLaughlin, D. Barford, Atomic structure of the APC/C and its mechanism of protein ubiquitination. *Nature* **522**, 450-454 (2015).
26. H. Labit *et al.*, Dephosphorylation of Cdc20 is required for its C-box-dependent activation of the APC/C. *EMBO J* **31**, 3351-3362 (2012).
27. N. Lianga *et al.*, A Wee1 checkpoint inhibits anaphase onset. *J Cell Biol* **201**, 843-862 (2013).
28. J. Y. Huang, G. Morley, D. Li, M. Whitaker, Cdk1 phosphorylation sites on Cdc27 are required for correct chromosomal localisation and APC/C function in syncytial Drosophila embryos. *J Cell Sci* **120**, 1990-1997 (2007).
29. I. Garcia-Higuera *et al.*, Genomic stability and tumour suppression by the APC/C cofactor Cdh1. *Nat Cell Biol* **10**, 802-811 (2008).
30. K. E. Gascoigne, S. S. Taylor, How do anti-mitotic drugs kill cancer cells? *J Cell Sci* **122**, 2579-2585 (2009).
31. A. W. Murray, Cell cycle extracts. *Methods Cell Biol* **36**, 581-605 (1991).
32. M. J. Hayes *et al.*, Early mitotic degradation of Nek2A depends on Cdc20-independent interaction with the APC/C. *Nat Cell Biol* **8**, 607-614 (2006).
33. H. Yamano, M. Trickey, M. Grimaldi, Y. Kimata, In vitro assays for the anaphase-promoting complex/cyclosome (APC/C) in Xenopus egg extracts. *Methods Mol Biol* **545**, 287-300 (2009).
34. K. Ohsumi, T. M. Yamamoto, M. Iwabuchi, Oocyte extracts for the study of meiotic M-M transition. *Methods Mol Biol* **322**, 445-458 (2006).
35. Y. Kimata, J. E. Baxter, A. M. Fry, H. Yamano, A role for the Fizzy/Cdc20 family of proteins in activation of the APC/C distinct from substrate recruitment. *Mol Cell* **32**, 576-583 (2008).
36. N. R. Brown *et al.*, CDK1 structures reveal conserved and unique features of the essential cell cycle CDK. *Nature communications* **6**, 6769 (2015).